DALTON
FULL PAPER

The synthesis and structure of a paramagnetic Lewis base adduct of antimony pentachloride, *trans*-[Mn^{II}(CNSbCl$_5$)(CO)$_2${P(OEt)$_3$}(dppm)][SbCl$_6$] †

Dena Bellamy, Nathan C. Brown, Neil G. Connelly * and A. Guy Orpen *

School of Chemistry, University of Bristol, Bristol, UK BS8 1TS

Received 29th March 1999, Accepted 19th July 1999

Treatment of *cis*-[Mn(CN)(CO)$_2${P(OEt)$_3$}(dppm)] with SbCl$_5$ gave paramagnetic *trans*-[Mn(CNSbCl$_5$)(CO)$_2${P(OEt)$_3$}(dppm)][SbCl$_6$] the crystal structure of which shows the geometry of the [Mn(CN)(CO)$_2${P(OEt)$_3$}(dppm)] fragment to be characteristic of a low-spin manganese(II) centre. The Mn–P(OEt)$_3$ and Mn–P$_{dppm}$ bond lengths are increased by 0.10 and 0.07 Å compared with those in analogous manganese(I) species while the Mn–C distances are little changed. A Cambridge Structural Database study of octahedral L·SbCl$_5$ species indicated that the Sb–Cl distances (*cis* and *trans* to the ligand L) and the average L–Sb–Cl$_{cis}$ angle are strongly correlated and appear to reflect the donor ability of the ligand L. A comparison of the geometry of the Mn(CNSbCl$_5$) moiety with those of other L·SbCl$_5$ species showed that the manganese ligand is a donor comparable with a range of other nitrogen and oxygen ligands but much weaker than ligands such as the phenyl anion. The geometry variations were analysed using a qualitative molecular orbital model for the bonding in L·SbCl$_5$ species.

Introduction

The complexes *trans*-[Mn(CN)(CO)$_2${P(OR)$_3$}(dppm)] (R = Et or Ph) have featured prominently as N-donor ligands in our studies of the construction and intramolecular electron-transfer reactions of bi- and poly-nuclear cyanide-bridged complexes.[1–5] These ligands are prepared[2] *via* the oxidatively induced isomerisation of the thermodynamically favoured isomer *cis*-[Mn(CN)(CO)$_2${P(OR)$_3$}(dppm)], either by treatment with [N(C$_6$H$_4$Br-*p*)$_3$][PF$_6$] (generated *in situ* from N(C$_6$H$_4$Br-*p*)$_3$ and [NO][PF$_6$]) to give *trans*-[Mn(CN)(CO)$_2${P(OEt)$_3$}(dppm)][PF$_6$] or by using the more stable salt [N(C$_6$H$_4$Br-*p*)$_3$][SbCl$_6$] (prepared from N(C$_6$H$_4$Br-*p*)$_3$ and SbCl$_5$[6]) to give *trans*-[Mn(CN)(CO)$_2${P(OEt)$_3$}(dppm)][SbCl$_6$]; careful reduction of either salt with hydrazine hydrate gives the desired product. In an attempt to devise a more convenient and direct synthetic route to *trans*-[Mn(CN)(CO)$_2${P(OEt)$_3$}(dppm)], avoiding the use of N(C$_6$H$_4$Br-*p*)$_3$ and expensive reagents such as [NO][PF$_6$], we have carried out the direct reaction of *cis*-[Mn(CN)(CO)$_2${P(OEt)$_3$}(dppm)] with SbCl$_5$ as the oxidant.[7] However, instead of the expected product, a salt of *trans*-[Mn(CN)(CO)$_2${P(OEt)$_3$}(dppm)]$^+$, we have isolated an unusual paramagnetic Lewis base adduct of SbCl$_5$, namely *trans*-[Mn(CNSbCl$_5$)(CO)$_2${P(OEt)$_3$}(dppm)][SbCl$_6$]. This species is of particular interest in enabling a comparison to be made of the structures of the (co-ordinated) redox pair *trans*-[Mn(CN)(CO)$_2${P(OEt)$_3$}(dppm)]^z ($z = 0$ or 1). Furthermore, we have compared the effect of the ligand [Mn(CN)(CO)$_2${P(OEt)$_3$}(dppm)]$^+$ on the geometry of the SbCl$_5$ moiety with those of other ligands, L, in complexes L·SbCl$_5$. The observed distortions are analysed using a qualitative molecular orbital approach.

Results and discussion

Synthesis of *trans*-[Mn^{II}(CNSbCl$_5$)(CO)$_2${P(OEt)$_3$}(dppm)][SbCl$_6$] 1

The reaction of *cis*-[Mn(CN)(CO)$_2${P(OEt)$_3$}(dppm)] with an excess of SbCl$_5$ in CH$_2$Cl$_2$ immediately gave an intense blue solution (rather than the red solution expected for the cation *trans*-[Mn(CN)(CO)$_2${P(OEt)$_3$}(dppm)]$^+$) from which deep blue crystals of **1** were isolated after addition of *n*-hexane to the reaction mixture and crystallisation of the resulting precipitate from CH$_2$Cl$_2$–*n*-hexane.

The presence of the low spin manganese(II) unit *trans*-[Mn(CO)$_2${P(OEt)$_3$}(dppm)]$^+$ in complex **1** was revealed by the one strong IR carbonyl band at 2010 cm^{-1} (*cf.* 1993 cm^{-1} for *trans*-[Mn(CN)(CO)$_2${P(OEt)$_3$}(dppm)]$^+$) and an anisotropic ESR spectrum almost identical to that of *trans*-[Mn(CN)(CO)$_2${P(OPh)$_3$}(dppm)]$^+$.[8] However, the presence of a band at 2136 cm^{-1} in the IR spectrum indicated the cyanide ligand to be bridging to an undefined Lewis acid the nature of which was only revealed by the X-ray structural analysis of **1**.

Structure of *trans*-[Mn^{II}(CNSbCl$_5$)(CO)$_2${P(OEt)$_3$}(dppm)][SbCl$_6$]·CH$_2$Cl$_2$

The unit cell of complex **1**·CH$_2$Cl$_2$ contains [Mn^{II}(CNSbCl$_5$)(CO)$_2${P(OEt)$_3$}(dppm)]$^+$ cations and [SbCl$_6$]$^-$ anions as well as dichloromethane of crystallisation. The structure of the cation is shown in Fig. 1 and selected bond lengths and angles are given in Table 1 and compared with those of related complexes of [Mn^I(CN)(CO)$_2${P(OEt)$_3$}(dppm)] in Table 2. The geometry around the manganese centre in **1** is essentially octahedral with the cyanide ligand also bound through N to an octahedral pentachloroantimony(V) centre; the Sb–N–C linkage is slightly bent [172.8(5)°]. The anion is separated from the cation in the solid by non-bonded distances greater than the sum of the van der Waals radii, except for one shorter CH···Cl distance [Cl(8)···H(16A) 2.788 Å], and occupies a

---

† *Supplementary data available*: CSD structural data for L·SbCl$_5$ species. For direct electronic access see http://www.rsc.org/suppdata/dt/1999/3191/, otherwise available from BLDSC (No. SUP 57615, 2 pp.) or the RSC Library. See Instructions for Authors, 1999, Issue 1 (http://www.rsc.org/dalton).

Table 1 Selected bond lengths (Å) and angles (°) for *trans*-[Mn^{II}(CNSbCl$_5$)(CO)$_2${P(OEt)$_3$}(dppm)][SbCl$_6$][a]

Mn–CN	1.959(7)
C–N	1.144(8)
Sb–N	2.180(6)
Mn–P(OEt)$_3$	2.319(2)
Sb–Cl$_{trans}$[b]	2.333(2)
Sb–Cl$_{cis}$[b] (average)	2.328(2)
Mn–CO	1.854(7), 1.866(7)
C–O	1.130(8), 1.127(8)
Mn–P$_{dppm}$	2.355(2), 2.356(2)
Sb–Cl (SbCl$_6$, average)	2.352(3)
Sb–N–C	172.8(5)
N–C–Mn	176.1(6)
O–P–O	109.0(3), 106.1(4), 100.7(3)
N–Sb–Cl$_{cis}$[b] (average)	86.1(2)
N–Sb–Cl$_{trans}$[b]	179.7(2)

[a] Estimated standard uncertainties for individual values are given in parentheses for the least significant digit, here and throughout this paper. [b] Refers to the position with respect to the Sb–N bond in the SbCl$_5$ moiety.

Table 2 Comparison of structural parameters (distances in Å, angles in °) for the Mn(CN)(CO)$_2${P(OEt)$_3$}(dppm) units in *trans*-[Mn^{II}(CNSbCl$_5$)(CO)$_2${P(OEt)$_3$}(dppm)][SbCl$_6$] **1** and complexes **2**–**4**[a]

Parameter	**1**	**2** (Rh)[3]	**3** (Au)[4]	**4** (Cd)[5]
Mn–P(OEt)$_3$	2.319(2)	2.215(6)	2.234(10)	2.223(2)
P–OEt	1.556(6)	1.600(14)	1.57(2)	1.594(5)
Mn–P$_{dppm}$	2.356(2)	2.291(5)	2.292(7)	2.288(2)
P–Ph$_{dppm}$	1.809(6)	1.811(16)	1.84(3)	1.832(7)
P–CH$_2$	1.835(6)	1.837(17)	1.86(3)	1.849(7)
Mn–CO	1.860(7)	1.830(17)	1.77(4)	1.834(8)
C–O	1.129(8)	1.132(19)	1.16(3)	1.153(8)
Mn–CN	1.959(7)	1.931(14)	1.95(3)	1.956(9)
C–N	1.144(8)	1.161(18)	1.12(3)	1.156(9)
O–P–O	105.3(4)	101.6(7)	99.9(13)	102.5(3)
C–P–C	107.1(3)	104.7(7)	104.6(12)	104.2(3)

[a] Dimensions are averaged where possible over equivalent parameters.

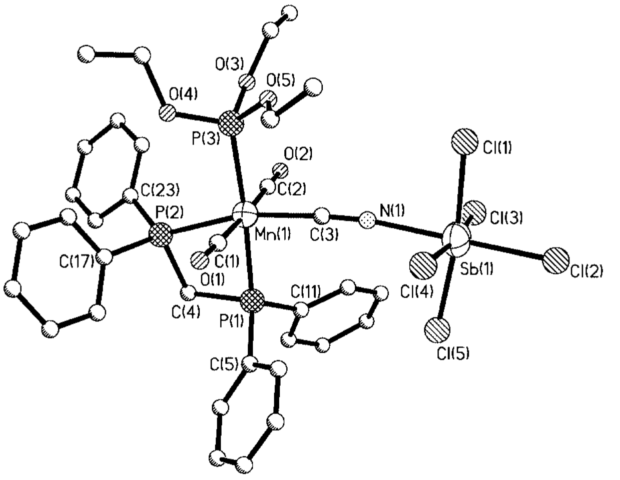

Fig. 1 Molecular structure of the cation of complex **1** showing atom labelling. Hydrogen atoms are omitted for clarity.

site in the region between the four dppm phenyl rings of one cyanomanganese ligand.

A comparison of the structures of *trans*-[Mn(CN)(CO)(dppm)$_2$]^z ($z = 0$ or 1) showed a large increase in the Mn–P distances (*ca.* 0.08 Å), accompanied by small but regular decreases in the P–C distances and increases in the C–P–C angles, on oxidation of Mn^I to Mn^{II}.[9] The different structural parameters for the two members of the redox pair are characteristic of the oxidation state of the manganese centre, even in species where the cyanomanganese complex acts as an N-donor ligand to a second metal site. Thus, the Mn–P bond distances are diagnostic of the manganese oxidation state in the redox pair [(OC)$_2$ClRh(μ-NC)Mn(CO)(dppm)$_2$]^z ($z = 0$, Mn^I; $z = 1$, Mn^{II}).[3]

The structural effects of oxidation on *trans*-[Mn(CN)(CO)$_2${P(OEt)$_3$}(dppm)] itself have not yet been quantified because it has so far proved impossible to crystallise a salt of the monocation *trans*-[Mn(CN)(CO)$_2${P(OEt)$_3$}(dppm)]$^+$. Such a comparison is of interest not only in providing a diagnostic structural measure of the oxidation state of such ligands, but also in shedding further light on the factors which affect intramolecular electron transfer in mixed valence complexes containing cyanomanganese(II) ligands. Extended Hückel molecular orbital and ESR spectroscopic studies[9] show that the SOMOs of the cations *trans*-[Mn(CN)(CO)(dppm)$_2$]$^+$ and *trans*-[Mn(CN)(CO)$_2${P(OEt)$_3$}(dppm)]$^+$ are δ and π with respect to the the Mn–CN axis so that mixed valence complexes of the former are likely to show less extensive intramolecular electron transfer between cyanide-linked redox centres.[3,4]

The structure of *trans*-[Mn(CNSbCl$_5$)(CO)$_2${P(OEt)$_3$}(dppm)]$^+$ is therefore of particular note as the first in which the geometry of the *trans*-[Mn^{II}(CN)(CO)$_2$L(L–L)]$^+$ (L, L–L = P donor ligands) unit is fully defined. It can therefore be compared (Table 2) with that of the neutral fragment *trans*-[Mn(CN)(CO)$_2${P(OEt)$_3$}(dppm)] which occurs in [Rh{(μ-NC)MnL$_x$}$_2$(CO)$_2$][PF$_6$] **2**,[3] [Au{(μ-NC)MnL$_x$}$_2$][PF$_6$] **3**[4] and [I$_2$Cd{(μ-NC)MnL$_x$}$_2$] **4**[5] [L$_x$ = *trans*-(CO)$_2${P(OEt)$_3$}(dppm)]. Thus, the Mn–P(OEt)$_3$ distance is longer in *trans*-[Mn(CNSbCl$_5$)(CO)$_2${P(OEt)$_3$}(dppm)]$^+$ **1** than in **2**–**4**, by *ca.* 0.10 Å. Similarly the Mn–P distances involving the dppm ligand are increased for the manganese(II) complex (by *ca.* 0.07 Å), while the Mn–CO distances increase only marginally [by 0.026 Å for **4**, the most precise of the manganese(I) structures] and the Mn–CN distance appears almost invariant. Accompanying the increases in the Mn–P distances on oxidation are reductions in P–O and P–C lengths and increases in O–P–O and C–P–C angles, as is expected given the importance of the σ* contribution to the π acceptor orbitals in phosphines and phosphites.[10] That the effects of oxidation of the manganese are focused at the phosphorus ligands is in accord with the molecular orbital model outlined above. Thus, the HOMO of the manganese(I) ligand is in the plane of the weaker π-acceptor ligands {the dppm, P(OEt)$_3$ and cyano ligands}, *i.e.* d$_{xy}$ if the OC–Mn–CO axis is taken as z. Therefore, depopulation of this orbital would be expected to lead to substantial decreases in Mn–P π bonding and no direct effect on the occupancy of the Mn–CO π-bonding orbitals (d$_{xz}$ and d$_{yz}$). The relative unimportance of Mn–CN π bonding, or at least the close balance between the bond lengthening due to loss of π bonding on metal oxidation and the bond shortening due to increased σ bonding, is perhaps surprising. Overall it is clear that structural parameters, notably those of the MnP$_3$ unit, can again be used to diagnose the manganese oxidation state (I or II) in complexes of *trans*-[Mn(CN)(CO)$_2${P(OEt)$_3$}(dppm)]^z ($z = 0$ or $+1$).

The structure of *trans*-[Mn(CNSbCl$_5$)(CO)$_2${P(OEt)$_3$}(dppm)]$^+$ may also be compared with those of [SbCl$_5$(NCMe)][11] (which is very imprecise, $R = 0.17$) and [SbCl$_5$(NCNPr$^i_2$)][12] (in which the contact nitrogen is not sp hybridised, Sb–N–C 133°) which show N–Sb and C–NSb bond lengths of 2.23 and 1.18 and 2.145 and 1.165 Å respectively, and with that of [SbF$_5$(NCCN)][13] for which the corresponding values are 2.214 and 1.123 Å.

The Sb–Cl bond length *trans* to the cyanomanganese ligand in complex **1** [2.333(2) Å] is essentially identical to the average Sb–Cl$_{cis}$ distance [2.328(3) Å] and both Sb–Cl distances are shorter than those in the [SbCl$_6$]$^-$ anion in **1** implying some *trans* (and *cis*) influence variation between Cl$^-$ and the cyanomanganese ligand. This is not an isolated example but

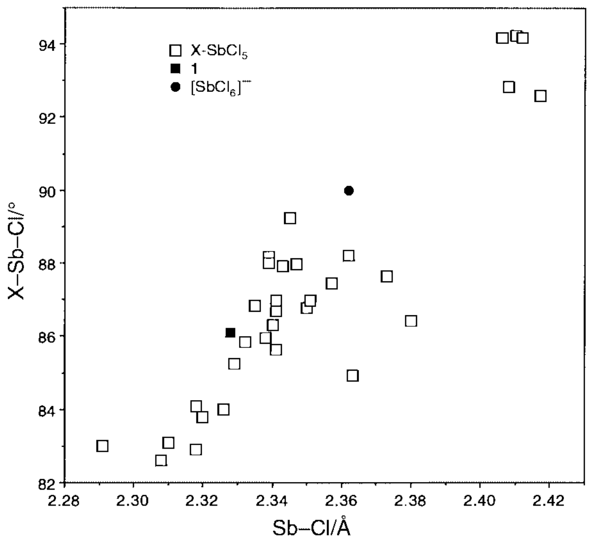

Fig. 2 Scatterplot of $\langle$Sb–Cl$_\mathrm{c}\rangle$ *vs.* α (X–Sb–Cl) for L·SbCl$_5$, [SbCl$_6$]$^-$ and complex **1**.

reflects the general behaviour in L·SbCl$_5$ species as discussed below.

The availability of structural data on other L·Sb$^\mathrm{V}$Cl$_5$ adducts through the Cambridge Structural Database (CSD)[14] prompted us to consider a study of the relative ability of ligands L to distort the SbCl$_5$ fragment. In the ubiquitous [SbCl$_6$]$^-$ anion the SbCl distances are, at least in principal,[15,16] all equal (and average 2.362 Å in 101 observations of good precision in the CSD) and the *cis* Cl–Sb–Cl angles average 90° while in **1** the *cis* N–Sb–Cl angles average 86.1°. In the 32 other L·SbCl$_5$ fragments available in the CSD there is considerable variation in the *cis*-Z–Sb–Cl angle (α, where Z is the contact atom of the ligand L) with average values ranging from 82.6 to 94.2°; there is corresponding variation in both the average *cis*-Sb–Cl ($\langle$Sb–Cl$_\mathrm{c}\rangle$) and *trans*-Sb–Cl (Sb–Cl$_\mathrm{t}$) distances (ranges 2.29–2.42 and 2.28–2.44 Å). These variations are closely coupled, as shown in Fig. 2 for α and $\langle$Sb–Cl$_\mathrm{c}\rangle$. Indeed, all three parameters, α, $\langle$Sb–Cl$_\mathrm{c}\rangle$ and Sb–Cl$_\mathrm{t}$ are significantly positively correlated in this data set (Spearman rank correlation coefficients $\rho_\mathrm{S} = 0.813$, 0.839 and 0.804 for the correlations between α and $\langle$Sb–Cl$_\mathrm{c}\rangle$, α and Sb–Cl$_\mathrm{t}$ and $\langle$Sb–Cl$_\mathrm{c}\rangle$ and Sb–Cl$_\mathrm{t}$ respectively).[17] At least part of the variation away from the ideal behaviour must be due to experimental uncertainties and variations in the temperature of data collection, but the general trend is clear.

Apparently the stronger donors (*i.e.* more basic) L cause more substantial increases in the Sb–Cl distances and the angle α in the L·SbCl$_5$ species in this dataset. Thus, all those structures with $\alpha > 90°$ have L = Ph$^-$ while those at the other extreme of the plot (to the lower left of Fig. 2) have weak O-donor ligands (such as C=O with electron withdrawing groups attached to the carbon). The amount of distortion (of α, $\langle$Sb–Cl$_\mathrm{c}\rangle$ or Sb–Cl$_\mathrm{t}$) from the values for [SbCl$_6$]$^-$ (90°, 2.362 and 2.362 Å) may therefore be tentatively taken as a structural measure of the donor ability of a ligand relative to that of Cl$^-$. From this viewpoint the manganese(II) ligand in **1** is a donor near the midpoint of the weaker ligand class which predominates in this data set (these are for the most part oxygen donors such as carbonyls and ylidic oxides of phosphorus or sulfur; in total there are 21 complexes with Z = O, six with Z = N, and five with Z = C) and rather weaker than chloride (Z = Cl, *i.e.* the [SbCl$_6$]$^-$ anions) or aryl anions (where Z = C).

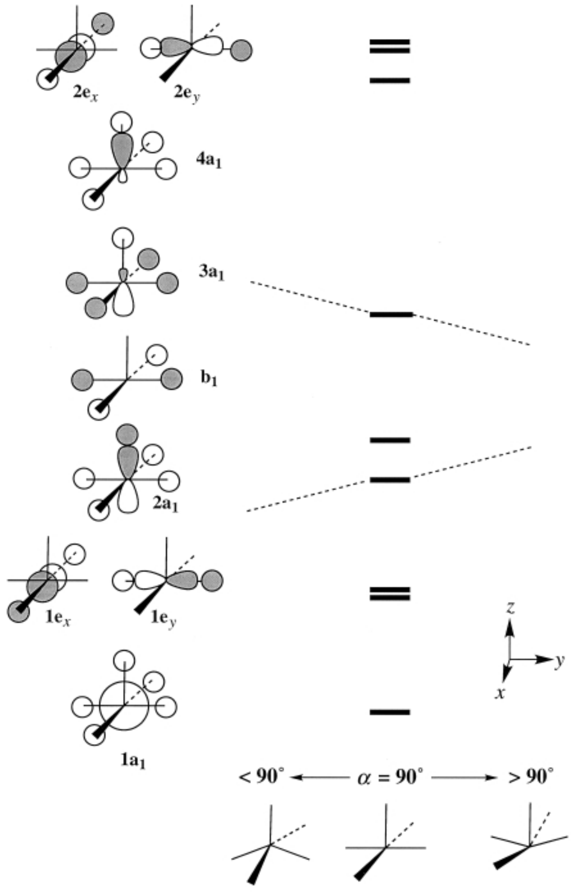

Fig. 3 Walsh diagram for SbCl$_5$ (or SbH$_5$) with $C_{4\mathrm{v}}$ symmetry indicating schematically the energy variation for the principal orbital interactions as a function of the angle α. The 3a$_1$ orbital is the LUMO.

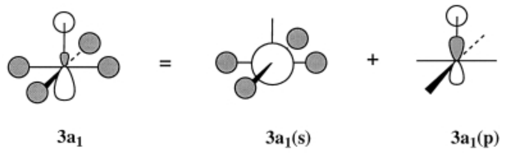

Fig. 4 The principal orbital interactions in the 3a$_1$ orbital of SbCl$_5$ (or SbH$_5$) with $C_{4\mathrm{v}}$ symmetry.

One might ask whether it is reasonable to assign these changes in the geometry of the SbCl$_5$ fragment to electronic effects. Fig. 3 shows schematically the variation in orbital energies for the key orbitals (2a$_1$ and 3a$_1$ for a $C_{4\mathrm{v}}$ symmetric SbCl$_5$ fragment, based on those provided for $C_{4\mathrm{v}}$ symmetric AB$_5$ species in refs. 18 and 19, and confirmed by extended Hückel calculations on SbH$_5$).[20] The 3a$_1$ orbital is the LUMO of SbCl$_5$ and is generally Sb–Cl antibonding, as illustrated in Fig. 4. This is confirmed by the bond lengths in the nine precisely determined [SbCl$_5$]$^{2-}$ anions in the CSD for which mean values of α (or its equivalent, there being no ligand atom Z but rather a lone pair), $\langle$Sb–Cl$_\mathrm{c}\rangle$ and Sb–Cl$_\mathrm{t}$ are 92.0°, 2.643 and 2.394 Å respectively (*i.e.* mean Sb–Cl 2.593 Å, *cf.* mean Sb–Cl in SbCl$_5$ 2.31 Å[21]). In a sense the [SbCl$_5$]$^{2-}$ anion is an extreme example of electron donation to the antimony in L·SbCl$_5$ species, *i.e.* the case in which L is an electron pair. At the other extreme lies the case where L is absent, *i.e.* that of SbCl$_5$. In practice, the geometry of SbCl$_5$ is trigonal bipyramidal and not square pyramidal as would be required for strict comparability with the octahedral complexes L·SbCl$_5$ or square pyramidal [SbCl$_5$]$^{2-}$. It is therefore instructive to consider the geometry of the [ECl$_5$]$^{2-}$ (E = In or Tl) ions which are isoelectronic with SbCl$_5$ but which *are* square pyramidal. In the case of [TlCl$_5$]$^{2-}$ the values of α, $\langle$Tl–Cl$_\mathrm{c}\rangle$ and Tl–Cl$_\mathrm{t}$ are 76.9°, 2.515 and 2.444 Å respectively[22] (although we note that effects of relativity for Tl may have distorting effects on these lengths). This implies that the weakest possible ligands L would give values of α approaching 80°, a value not inconsistent with the appearance of Fig. 2.

In general it is clear that the X ligand and the *trans* chloride in these species are competing for the same orbitals at Sb (see ref. 23). This is of course the origin of the *trans* influence in these and related species. In so far as the antimony 5s orbital is involved, the X ligand will also be in competition with the *cis* Cl ligands and have *cis* influence. Thus the observed correlations are as would be expected since rehybridisation (*i.e.* $\alpha > 90°$ for donors stronger than Cl and <90° for donors weaker than Cl) would maximise the Sb to better donor interaction. A qualitative model for this behaviour may be advanced based on the Walsh diagram shown in Fig. 3. At its simplest (and ignoring perturbations to the orbital pattern arising from X–Sb interaction) we may treat those geometrical variations (in α and bond lengths) arising from electronic effects by considering the occupancy of the $3a_1$ orbital in Fig. 3. Putting electrons in to this orbital produces a driving force for a geometry with $\alpha > 90°$ as a result of antibonding overlap of the equatorial terminal atom (Cl in $SbCl_5$, or H in SbH_5) orbitals with the antimony p_z orbital [see $3a_1$(p) in Fig. 4]. The operation of this driving force is consistent with the α values observed in $[SbCl_5]^{2-}$ (92°) or the isoelectronic BrF_5 (96°),[24] while for the strongest donors present here ($L = Ph^-$) $\alpha = 94°$. Holding the occupancy of $3a_1$ at zero or only just above (as for weak donors L) would be expected to lead to $\alpha < 90°$. This geometry allows for stabilisation of the $2a_1$ orbital as a result of bonding interactions between the antimony p_z orbital and the equatorial terminal atoms (see Fig. 3), and the minimisation of unfavourable *cis* Cl···Cl contacts. This geometry is observed in **1** and in $[TlCl_5]^{2-}$. Certainly, steric effects must also play a role although it is hard to see how these can be large for the linear RCN ligands of **1** or $[SbCl_5(NCMe)]$ for example. Overall, therefore, it seems that an electronic explanation for the observed correlations is likely and that geometric distortions in $L{\cdot}SbCl_5$ species may be used as a measure of the donor ability of L.

Surprisingly, the cyclic voltammogram of *trans*-$[Mn(CNSbCl_5)(CO)_2\{P(OEt)_3\}(dppm)][SbCl_6]$ could not be recorded. Although the complex is stable in CH_2Cl_2 in the absence of air, it decomposes to *trans*-$[Mn(CN)(CO)_2\{P(OEt)_3\}(dppm)]^+$ when added to a solution containing the supporting electrolyte $[NBu_4][PF_6]$ (which is usually regarded as inert!). Solutions of *trans*-$[Mn(CNSbCl_5)(CO)_2\{P(OEt)_3\}(dppm)][SbCl_6]$ in CH_2Cl_2 do not react with either $[NBu_4]I$ or $[NBu_4][BF_4]$ but do so with $[CoCp_2][PF_6]$, implicating the $[PF_6]^-$ anion rather than the $[NBu_4]^+$ cation in the decomposition process. It is possible that *trans*-$[Mn(CNSbCl_5)(CO)_2\{P(OEt)_3\}(dppm)][SbCl_6]$ is stabilised in solution as a close ion pair. In the presence of an excess of the $[PF_6]^-$ anion, ion separation may result, allowing dissociation of the cation *trans*-$[Mn(CNSbCl_5)(CO)_2\{P(OEt)_3\}(dppm)]^+$ into $SbCl_5$ and *trans*-$[Mn(CN)(CO)_2\{P(OEt)_3\}(dppm)]^+$.

The formation of *trans*-$[Mn(CNSbCl_5)(CO)_2\{P(OEt)_3\}(dppm)]^+$ might occur by two pathways, namely (i) oxidation of *cis*-$[Mn(CN)(CO)_2\{P(OEt)_3\}(dppm)]$ to *trans*-$[Mn(CN)(CO)_2\{P(OEt)_3\}(dppm)]^+$ followed by co-ordination of $SbCl_5$ at N, or (ii) co-ordination of $SbCl_5$ at N and subsequent oxidation of *cis*-$[Mn(CNSbCl_5)(CO)_2\{P(OEt)_3\}(dppm)]$. The complex *trans*-$[Mn(CN)(CO)_2\{P(OEt)_3\}(dppm)][PF_6]$ does indeed react with an excess of $SbCl_5$ to give *trans*-$[Mn(CNSbCl_5)(CO)_2\{P(OEt)_3\}(dppm)]^+$. However, the IR spectrum of a solution containing *cis*-$[Mn(CN)(CO)_2\{P(OEt)_3\}(dppm)]$ and a deficiency of $SbCl_5$ shows the presence of a mixture of *trans*-$[Mn(CNSbCl_5)(CO)_2\{P(OEt)_3\}(dppm)]^+$, *trans*-$[Mn(CN)(CO)_2\{P(OEt)_3\}(dppm)]^+$, and a third product with bands at 1976 and 1936 cm^{-1}. This third product may be *cis*-$[Mn(CNSbCl_5)(CO)_2\{P(OEt)_3\}(dppm)]$ given that an increase in ν(CO) is expected on co-ordination at N (*cis*-$[Mn(CN)(CO)_2\{P(OEt)_3\}(dppm)]$ shows carbonyl absorptions at 1954 and 1894 cm^{-1}).

Experimental

The preparation of the new complex was carried out under an atmosphere of dry nitrogen using dried, distilled and deoxygenated solvents; the reaction was monitored by IR spectroscopy. The compound *cis*-$[Mn(CN)(CO)_2\{P(OEt)_3\}(dppm)]$[2] was prepared by the published method; $SbCl_5$ was purchased from Aldrich. The IR spectra were recorded on a Nicolet 5ZDX FT spectrometer. Microanalyses were carried out by the staff of the Microanalytical Service of the School of Chemistry, University of Bristol.

Synthesis of *trans*-$[Mn(CNSbCl_5)(CO)_2\{P(OEt)_3\}(dppm)][SbCl_6]$

Liquid $SbCl_5$ (*ca.* 110 µL, 0.868 mmol) was added dropwise to a stirred solution of *cis*-$[Mn(CN)(CO)_2\{P(OEt)_3\}(dppm)]$ (100 mg, 0.145 mmol) in CH_2Cl_2 (20 cm^3). The dark blue solution was filtered and *n*-hexane added. The volume of the mixture was reduced *in vacuo* until a blue powder was obtained. Layering *n*-hexane onto a CH_2Cl_2 solution of the product gave deep blue crystals, yield 62 mg (32%). Found (Calc.): C, 31.0 (30.9); H, 3.0 (2.8); Cl, 28.7 (29.6); N, 1.0 (1.1)%. IR(CH_2Cl_2): ν(CN), 2136mw; ν(CO), 2010s cm^{-1}. The solid is moderately stable in air but decomposes slowly in solution to give *trans*-$[Mn^{II}(CN)(CO)_2\{P(OEt)_3\}(dppm)]^+$.

Structure determination of *trans*-$[Mn^{II}(CNSbCl_5)(CO)_2\{P(OEt)_3\}(dppm)][SbCl_6]{\cdot}CH_2Cl_2$

Blue crystals suitable for X-ray diffraction studies were obtained by allowing a concentrated CH_2Cl_2 solution of complex **1** to diffuse into *n*-hexane at −10 °C. The structure analysis was carried out by standard area detector methods.

Crystal data. $C_{35}H_{39}Cl_{13}MnNO_5P_3Sb_2$, $M = 1405.9$, monoclinic, space group $P2_1/n$ (no. 14), $a = 16.267(3)$, $b = 13.822(3)$, $c = 24.993(5)$ Å, $\beta = 97.95(3)°$, $V = 5566(2)$ Å^3, $T = 293$ K, $Z = 4$, $D_x = 1.678$ g cm^{-3}, $\mu = 1.93$ mm^{-1}, 21246 reflections measured, 7940 unique, $R_{int} = 0.0321$, $R1 = 0.0476$. Unresolved disorder led to very anisotropic ellipsoids of the phosphite ligand substituents and prevented satisfactory anisotropic refinement of C(34).

CCDC reference number 186/1582.

See http://www.rsc.org/suppdata/dt/1999/3191/ for crystallographic files in .cif format.

Database study

Geometric data for $ZSbCl_5$ fragments ($Z \neq Cl$) and $[SbCl_6]^-$ anions (the latter for those 81 structures without disorder and with $R < 0.05$) were retrieved from the October 1998 version of the Cambridge Structural Database.[14] Average Sb–Cl distances *cis* to Z (⟨$Sb–Cl_c$⟩), Sb–Cl distances *trans* to Z ($Sb–Cl_t$), and average *cis*-Z–Sb–Cl bond angles α were calculated for each case, and for $[SbCl_6]^-$ the average of all the ⟨Sb–Cl⟩ values was taken. The CSD refcodes and molecular dimensions for the fragments shown have been deposited (SUP 57615). Extended Hückel calculations were carried out using the CaChe package[20] with standard parameters and idealised geometry for the SbH_5 fragment.

Acknowledgements

We thank the EPSRC for a Research Studentship (to N. C. B.) and a referee for helpful comments.

References

1 A. Christofides, N. G. Connelly, H. J. Lawson, A. C. Loyns, A. G. Orpen, M. O. Simmonds and G. H. Worth, *J. Chem. Soc., Dalton Trans.*, 1991, 1595; F. L. Atkinson, N. C. Brown, N. G. Connelly, A. G. Orpen, A. L. Rieger, P. H. Rieger and G. M. Rosair, *J. Chem. Soc., Dalton Trans.*, 1996, 1959; N. G. Connelly, O. M. Hicks, G. R. Lewis, A. G. Orpen and A. J. Wood, *Chem. Commun.*, 1998, 517; N. G. Connelly, O. M. Hicks, G. R. Lewis, M. T. Moreno and A. G. Orpen, *J. Chem. Soc., Dalton Trans.*, 1998, 1913.

2 G. A. Carriedo, N. G. Connelly, M. C. Crespo, I. C. Quarmby, V. Riera and G. H. Worth, *J. Chem. Soc., Dalton Trans.*, 1991, 315.

3 F. L. Atkinson, A. Christofides, N. G. Connelly, H. J. Lawson, A. C. Loyns, A. G. Orpen, G. M. Rosair and G. H. Worth, *J. Chem. Soc., Dalton Trans.*, 1993, 1441.

4 N. C. Brown, G. B. Carpenter, N. G. Connelly, J. G. Crossley, A. Martin, A. G. Orpen, A. L. Rieger, P. H. Rieger and G. H. Worth, *J. Chem. Soc., Dalton Trans.*, 1996, 3977.

5 N. G. Connelly, G. R. Lewis, M. T. Moreno and A. G. Orpen, *J. Chem. Soc., Dalton Trans.*, 1998, 1905.

6 F. A. Bell, A. Ledwith and D. C. Sherrington, *J. Chem. Soc. C*, 1969, 2719.

7 N. G. Connelly and W. E. Geiger, *Chem. Rev.*, 1996, **96**, 877.

8 N. G. Connelly, K. A. Hassard, B. J. Dunne, A. G. Orpen, S. J. Raven, G. A. Carriedo and V. Riera, *J. Chem. Soc., Dalton Trans.*, 1988, 1623.

9 G. A. Carriedo, N. G. Connelly, E. Perez-Carreno, A. G. Orpen, A. L. Rieger, P. H. Rieger, V. Riera and G. M. Rosair, *J. Chem. Soc., Dalton Trans.*, 1993, 3103.

10 A. G. Orpen and N. G. Connelly, *Organometallics*, 1990, **9**, 1206.

11 H. Binas, *Z. Anorg. Allg. Chem.*, 1967, **352**, 271.

12 J. C. Jochims, R. Abu-El-Halawa, L. Zsolnai and G. Huttner, *Chem. Ber.*, 1984, **117**, 1161.

13 I. C. Tornieporth-Oetting, T. M. Klapotke, T. S. Cameron, J. Valkonen, P. Rademacher and K. Kowski, *J. Chem. Soc., Dalton Trans.*, 1992, 537.

14 F. H. Allen, J. E. Davies, J. J. Galloy, O. Johnson, O. Kennard, C. F. Macrae, E. M. Mitchell, G. F. Mitchell, J. M. Smith and D. G. Watson, *J. Chem. Inf. Comput. Sci.*, 1991, **31**, 187.

15 G. A. Landrum and R. Hoffmann, *Angew. Chem., Int. Ed.*, 1998, **37**, 1887.

16 A. Martín and A. G. Orpen, *J. Am. Chem. Soc.*, 1996, **118**, 1464.

17 B. J. Dunne, R. B. Morris and A. G. Orpen, *J. Chem. Soc., Dalton Trans.*, 1991, 653.

18 B. M. Gimarc, *Molecular Structure and Bonding*, Academic Press, New York, 1979.

19 T. A. Albright, J. K. Burdett and M.-H. Whangbo, *Orbital Interactions in Chemistry*, Wiley, New York, 1985.

20 CaChe Worksystem, CaChe Scientific, Beaverton, OR, 1994.

21 G. L. Carlson, *Spectrochim. Acta*, 1963, **19**, 1291.

22 M. A. James, M. B. Millikan and B. D. James, *Main Group Metal Chem.*, 1991, **14**, 1.

23 N. Kaltsoyannis and P. Mountford, *J. Chem. Soc., Dalton Trans.*, 1999, 781; P. D. Lyne and D. M. P. Mingos, *J. Chem. Soc., Dalton Trans.*, 1995, 1635; J. K. Burdett and T. A. Albright, *Inorg. Chem.*, 1979, **18**, 2112; E. M. Shustorovich, M. A. Porai-Koshits and Y. A. Buslaev, *Coord. Chem. Rev.*, 1975, **17**, 1.

24 A. G. Robiette, R. H. Bradley and P. N. Brier, *Chem. Commun.*, 1971, 1567.

Paper 9/02481F